Study of MHD SWCNT-Blood Nanofluid Flow in Presence of Viscous Dissipation and Radiation Effects through Porous Medium

M. Ramanuja[a,b,*], J. Kavitha[c], A. Sudhakar[a], V. NagaRadhika[b]

[a]*Department of Mathematics, Marri Laxman Reddy Institute of Technology and Management, Dundigal, Hyderabad – 500 043, India*
[b]*Department of Mathematics, GITAM Institute of Technology and Management, Bangalore, Karnataka – 561203, India*
[c]*Department of Mathematics D K, Government College for Women, SPSR Nellore-524003, India*

Abstract

In this analysis, a computational study is conducted to examine the two-dimensional flow of an incompressible MHD SWCNT-blood nanofluid, saturated mass and porous medium .In addition to viscous dissipation, thermal radiation is taken into consideration. We developed the mathematical model and useful boundary intensity approximations to diminish the structure of partial differential equations based on the fluid for blood-based SWCNT underflow assumptions. Converted the partial differential equations by applying corresponding transformations to arrive at ODE's. The above results are solved numerically by the Runge-Kutta 4th order technique. Noticed that there is desirable conformity when interpolated with the numerical one. The effects exhibited the velocity of SWCNT-blood nanofluid enhanced for defined standards of the viscosity parameter. Rise in temperature when various parameters like Prandtl number, Eckert number, and slip parameter are applied on SWCNT-blood. The impact of fluid flow on blood-based SWCNT is discussed graphically, and our results are tabulated along with illustrations. The design concepts, such as the Nusselt quantity and the local skin friction, conform to the analytical approach. Velocity reductions with an increase in CNT's volume fraction, whereas enhancement in the blood temperature, is noted, which is directed to the rise in the heat mass transfer rates.

Communicated by: S. Fadugba

1. Introduction

The study of non-Newtonian fluids like water, mineral oil, and ethylene glycol was reported in many papers for more than a decade, and their applications could be found in industrial sectors such as chemical manufacturing, microelectronics, air conditions, engineering, petroleum industry, paper production, aerodynamic heating, coating, and polymer processing, etc. A range of substances such as blood, mud, polymers, and paint depicts a non-Newtonian fluid description. However, no single model in literature deals with multiple non-Newtonian fluids. But the properties of these fluids are multiple in themselves because of their low thermal conductivity, which hampers their functions during heat exchangers. As a consequence, there may be a demand to expand its thermal conductivity. In contempo-

---

*Corresponding author tel. no: +91 9550754250
Email address:* mramanuja09@gmail.com (M. Ramanuja)

rary applications, due to commercial aspects, the flow involving Casson nanofluid creates critical interest in present-day researchers. Many substances in the actual field, like mud, malt, condensed milk, glues, sugar solution, emulsions, soaps, paints, etc., exhibit Newtonian fluid properties. But the actual situation is to assemble a single constitutive equation that follows the defined Casson nano -fluid's properties. It also plays a vital function in nuclear physics within geographical flows. Many researchers have identified different effects resting on Casson nanofluid.

Salman et al. [1] developed a combination of viscous dissipation with radiation parameters. The cone angle has a significant result on heat transfer and fluid flow conduct within the porous medium. The consequences of viscous dissipation, holmic dissipation, thermal radiation, and mass exchange outcomes on uneven hydromagnetic boundary thickness float of a stretching plane were developed by Anjali Devi et al. [2]. Abd El Aziz [3] is interested in the impact of thermal radiation along with mixed heat and mass transfer on hydromagnetic with the flow over a porous stretching level. MHD float was scientifically clarified with radiation via a stretching sheet surrounded by a porous medium, as specified and examined by Anjali et al. [4]. Makinde et al. [5] have analyzed the chemical response results from the stretching surface in the existence of interior heat invention. The radiation and chemical response outcomes on the MHD boundary layer glide of a stretching surface were examined by Seini et al. [6]. Abdul et al. [7] have investigated, via a stretching flat surface, the effect of thermal radiation on MHD fluid flow. The pressure of thermal radiation on the MHD flow via the stretching surface was discussed by Chen et al. [8]. Further, Raju et al. [9] concentrated on resting the movement of Casson fluid through a slippery wedge and noticed a decrease in the increasing temperature area estimations of the Eckert number.

Electrically directing Casson liquid flow over an item that is neither a perfect level/vertical slanted/cone in the presence of a steady, attractive field is also a significant concern. Sabetha et al. [10] determined the thermal radiation results on hydromagnetic free convection drift previously and impetuously began vertical plate. Hiteesh [11] studied the absence of transverse magnetic discipline, the border layer regular drift and heat transfer of a viscous incompressible fluid resulting from stretching plate with viscous dissipation impact.

The convection heat transfer side by way of a constantly shifting heated vertical plate, including suction or injection analyzed by Al-Sanea [12]. Unsteady free convection and mass change glide over a limitless vertical permeable plate in the commentary of suction/injection are to come upon with learning about by Takhar et al. [14]. The impact of suction /injection on unsteady free convection Couette float and warmth switch of an active viscous fluid with vertical permeable plate is explained by Jha et al. [16].

Shamshuddin et al. [17] developed a particular cover of flow that isn't dissipative, and in-depth graphical illustrations are offered for the fine of the magnetic subject parameter. Further, Shah et al. employed the dissimilar case of nanoparticles. Additionally, entropy optimization with activation elec-

tricity and chemical response is also studied. The 2nd regulation of Thermodynamics is utilized to discover the entropy technology in velocity. Heat and mass switch of Williamson nanofluid causes a magnetohydrodynamic perimeter layer to move with the flow across a stretched sheet explored by Reddy et al. [19]. The magnetohydrodynamic (MHD) flow of Casson nanofluid impact over an extended surface was developed by Hayat et al. [20]. Dawar et al.[22] investigated the MHD Casson-nanofluid, carbon nanotube, and radioactive heat transfer revolving channels. Ali et al. [21] studied the blood moves with the Casson fluid below the influence of MHD magnetohydrodynamics in axis-symmetric cylindrical tubes.

The MHD Williamson fluid via a bent sheet and below the influence of non-thermal heat source or sink CNTs is analyzed by Kumar et al. [23]. C. Sus [24] for the first time, nanofluids were proposed by elevating nanometer and sized particles interested in the bottom fluid. The (SWCNTs) single-walled carbon annotates own a better heat transfer assessment, and surface drag compels (MWCNTs) multiwall carbon annotates described by Haq et al. [25]. Further, Liu et al. [26] examined glycol, ethylene, and engine oil with the existence of MWCNTs, and they concluded that CNTs with ethylene glycol have an advanced thermal conductivity. Recently, The approach of nanofluid precedent above a stretching sheet was obtained by Needed and Lee [27]. The boundary deposit flow of nanoparticles concluded a stretching/shrinking exterior had been examined by Nadeem Bejan [28].

Further, Hayat et al.[29] obtained the nonmaterial fluid flow in a circulating method. The nanofluid flow throughout the entropy generation considers the circular heat source, which is studied by Nouri et al. [30]. Das et al. [31] have analyzed the MHD flow of nanofluid through a porous medium. Further, Sheremet et al. [32] examined the identical fluid in the crimped cavity. The flow of nanofluid in an enlarged porous sheet is observed by Alharbi et al. [33]. Zueco[34] exploited a community simulation technique (NSM) to check the consequences of viscous dissipation and radiation on unsteady free convection MHD on a vertical porous plate. Hamzeh et al. [45] aims to investigate the properties of heat transfer and magnetohydrodynamics Casson nanofluid in the presence of a free convection boundary layer fluid flow on a stretching sheet using CNTs in human water/blood as the base fluid.

The unsteady separated stagnation-point flow of hybrid nanofluid with viscous dissipation and Joule heating is investigated numerically in this examined by Amira Zainal et al. [46]. Zainal et al. [47] have investigated viscous dissipation and MHD hybrid nanofluid flow towards an exponentially stretching/shrinking surface. Taza et al. [48] have studied heat and mass transmission more conveniently, such as in hybrid-powered engines, pharmaceutical processes, microelectronics, domestic refrigerators, and engine cooling. Aditya et al. [49] have been examined by considering Buongiorno's two-component non-homogeneous model with the inclusion of electrification of nanoparticles and viscous dissipation. Adedire et al. [50] examined the concentration profiles in the single and the interconnected multiple-compartment systems with sievepartitions to transport chemical species with second-order chemical re-

action kinetics. Ramanuja et al. [51] have examined Casson nanofluid flow over a growing or contracting porous medium with different permeability and thermal radiation.[54] have obtained numerical experiments show that the methods compete favourably with existing processes and efficiently solve stiff and oscillatory problems.

Nanofluids are obtained by reacting oxides, metals, carbides, or carbon nanotubes (CNTs) with nanoparticles. Generally, in base fluids, nanoparticles are regularly floating, consisting of water, kerosene, ethylene glycol, and engine oil in some areas. CNTs used inner nanofluids, which are available in two types in carbon nanotubes (SWCNTs), and colloidal deferment of nanoparticles in a base fluid is used to create these fluids.

This model investigates the stagnation flow on SWCNT and blood nanofluids of MHD fluid in the existence of a porous medium, viscous dissipation, and investigation under the impact of injection/suction in addition to thermal radiation parameters are studied and analyzed through this examination. Numerical techniques solved the resulting equations. Symbolic computational software such as MATLAB bvp4c solver is used. The effects are presented graphically.

2. Formation of the Problem

The physical description of the problem is illustrated in fully-developed steady-mixed convection flow of human blood utilized as base fluid, and SWCNT as the nanoparticles over a state, incompressible, laminar flow of SWCNT-based nanofluids saturated with human blood is embedded in the medium porous surface that allows the liquid to enter or exit during progressive developments or constrictions. The porous plates are separated by distance a. One part of the cross-segment converse to separation by $2a$ (t)between the walls, which is to a great extent less than the channel's width and length. A consistent segment of the flow field is shown in the Cartesian coordinate system, which is chosen within such a manner as exposed in fig.1. One and the other channel partitions are perceived to have distinct permeability issues and expansion or convention are systematically at a dependents-time velocity $v_0$which represents the uniform suction $v_0 > 0$ and injection $v_0 < 0$channel which is supposed to be infinite in the distance. Because of their magnetic characteristics, these nanoparticles are considered. In the proposed issue, the Casson liquid model is exposed to blood and SWCNTs nanoparticles which are scattered into it for upgraded heat move.

The above assumptions portrays leading equations in support of the nanofluid flow by 2-dimensional boundary cover equations are assumed as a continuity equation, momentum equation, and the energy equations as mentioned by Vijayalakshmi *et al.* [41]; Bestman [42]; Srinivas *et al.* [43] and Radha krinshnama charya *et al.*[44].

$$\frac{\partial u}{\partial x} + \frac{\partial v}{\partial y} = 0 \qquad (1)$$
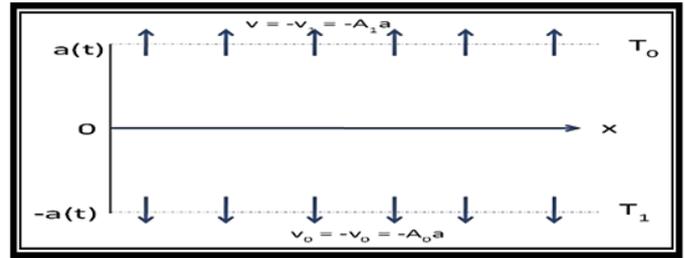
Figure 1. Schematic of problem

$$\frac{\partial u}{\partial t} + u\frac{\partial u}{\partial x} + v\frac{\partial u}{\partial y}$$

$$= \frac{\mu_{nf}}{\rho_{nf}}\left(1 + \frac{1}{\beta}\right)\left(\frac{\partial^2 u}{\partial x^2} + \frac{\partial^2 u}{\partial y^2}\right)$$

$$- \frac{\mu_{nf}\phi}{\rho_{nf}k}\left(1 + \frac{1}{\beta}\right)u - B_0^2\sigma_{nf}\frac{\mu_{nf}u}{\rho_{nf}} - \frac{1}{\rho_{nf}}\frac{\partial p}{\partial x} \quad (2)$$

$$\frac{\partial v}{\partial t} + u\frac{\partial v}{\partial x} + v\frac{\partial v}{\partial y}$$

$$= \frac{\mu_{nf}}{\rho_{nf}}\left(1 + \frac{1}{\beta}\right)\left(\frac{\partial^2 v}{\partial x^2} + \frac{\partial^2 v}{\partial y^2}\right)$$

$$- \frac{\mu_{nf}\phi}{\rho_{nf}k}\left(1 + \frac{1}{\beta}\right)v - B_0^2\sigma_{nf}\frac{\mu_{nf}u}{\rho_{nf}} - \frac{1}{\rho_{nf}}\frac{\partial p}{\partial y} \quad (3)$$

$$\frac{\partial T}{\partial t} + u\frac{\partial T}{\partial x} + v\frac{\partial T}{\partial y}$$

$$= \frac{k_{nf}}{(\rho_{C_P})_{nf}}\left(\frac{\partial^2 T}{\partial y^2}\right) - \frac{1}{(\rho_{C_P})_{nf}}\frac{\partial q_r}{\partial y} + \frac{\mu_{nf}}{(\rho_{C_P})_{nf}}\left(1 + \frac{1}{\beta}\right)\left(\frac{\partial u}{\partial y}\right)^2$$

$$+ \frac{q'''}{(\rho_{C_P})_{nf}} + \frac{Q_0}{(\rho_{C_P})_{nf}}(T - T_0) \quad (4)$$

where $u$and v denote the velocity fundamental quantities, with the directions of x-axis and$y$-axis, $p$denote the dimensional pressure t be the time,ϕ&k are the permeability and porosity of the permeable medium, ϕ (η) is the dimensionless concentration of the fluid, temperature T,k_{nf}denote the thermal conductivity of the nanofluid, β be the blood Casson fluid parameter,ρ_{nf}be the efficient density of the nanofluid, the efficient dynamic viscosity of the nanofluid be μ_{nf}, $(\rho_{C_P})_{nf}$ denote the heat electrical condenser of the nanofluid, and $v$denote the kinematic viscosity.

The non-uniform heat absorbed by generation per unit volume $q'''$is defined as:

$$q''' = \frac{B(x_0)^{m+1}k}{vx_0}[f^1(\eta)A^*(T_1 - T_0) + B^*(T - T_0)]$$

Here $_{A^*}$represents the velocity of heat transfer for the space-dependent and B^* represents an exponentially decaying parameter of space and internal temperature-dependent heat absorption.

where $A_0 = v_0 a^{-1}$ and $A_1 = v_1 a^{-1}$ are the wall permeability quantities;T_0, $T_1$are the temperature of the upper and lower

walls; T_w is the temperature taking place at the wall; T_∞ is the temperature of free stream fluid flow. The substantial effects of the such as nanofluid $\rho_{nf}, \mu_{nf}, (\rho C_P)_{nf}$, and k_{nf} are involved in the outcomes of the distance distribution on CNTs are compensated for using spinning oblique nanotubes with a very large axial ratio and given as, which might be outlined.

2.1. Mathematical Model for the Thermal Physcial Property of a Nanofluid

Table 1 Mathematical model for the thermal physical property of a nanofluid the viscosity, density, heat capacitance and the effective thermal conductivity of the nanofluid are defined as given by H.C. Brikman [52] and R. I. Hamilton *et al.* [53] respectively:

Where, *n*the nanoparticle is shape factor , $v_{nf} = \frac{\mu_{nf}}{\rho_{nf}}$,ϕ- the volume of the utility of nanoparticles,ρ_f - Concentration of the base fluid, ρ_s-be the density of the nanoparticle, μ_f-viscosity of the base fluid, $(\rho C_p)_f$, $(\rho C_p)_s$- The capacitance heat of the base fluid along with nanoparticle is a combination with solid nanoparticles, and k_f; $k_s$thermal conductivities of the base fluid and nanoparticle correspondingly. The thermo-physical properties of changed base fluids and nano-particles are revealed in Table 1. By introducing the complimentary flow utility, the same represents flow velocity components *u* and *v* can be written through conditions of the free flow function in flow.

$$u = \frac{\partial \psi}{\partial y} \quad and \quad v = -\frac{\partial \psi}{\partial x} \quad (5)$$

Partial differential equations that are non-linear and condensed addicted to non-linear ODE's deliberated for that purpose the stream function where$\psi = \psi(x, y)$routinely satisfy continuity equation, indicates stream function appropriate to mass conservation and $f(\eta)$ is dimensionless flow function.

$$u = xva^{-2}F_n(\eta, t), \quad v = -va^{-1}F(\eta, t) ; \psi = xvF(\eta, t)/a \quad (6)$$

Here $\eta = \frac{y}{a}$, $F_n = \frac{\partial F}{\partial \eta}$

The governing equations (2) are based on these assumptions are given by Vijayalakshmi *et al.* [41]:

$$\frac{\partial u}{\partial t} = \frac{\mu_{nf}}{\rho_{nf}} \left(1 + \frac{1}{\beta}\right) \frac{\partial^2 u}{\partial y^2} - \frac{\mu_{nf}\phi}{\rho_{nf} k} \left(1 + \frac{1}{\beta}\right) u - B_0^2 \sigma_{nf} \frac{\mu_{nf} u}{\rho_{nf}} - \frac{1}{\rho_{nf}} \frac{\partial p}{\partial x} \quad (7)$$

Usage of the irradiative heat flux is basic in Rosseland's estimate for radiation Brewster [39], and the thermal flux is defined as:

$$q_r = -\frac{4\sigma^*}{3k^*} \frac{\partial T^4}{\partial y} \quad (8)$$

Here and k^* be the "absorption Specific" coefficient, σ^*- be the Stefan-Boltzmann constant. We had been constrained that the temperature variations contained by using the glide are satisfactorily slighter such that the term T^4strength is stated as a direct function of temperature. This is consummated by increasing T^4

in Taylor's sequence about T_∞ and ignoring higher-order expressions, thus assuming a small temperature difference in flow given below:

$$T^4 \cong 4T_\infty^3 T - 3T_\infty^4 \quad (9)$$

Using Eqs(9) and Eqs(8) becomes

$$\frac{\partial q_r}{\partial y} = \frac{-16\sigma^* T_\infty^3}{3k^*} \frac{\partial^2 T}{\partial y^2} \quad (10)$$

Under these assumptions, the leading equations are given by Vijayalakshmi *et al.* [41]; Bestman [42]; Srinivas *et al.* [43]

$$\frac{\partial T}{\partial t} = \frac{k_{nf}}{(\rho C_P)_{nf}} \left(\frac{\partial^2 T}{\partial y^2}\right) + \frac{1}{(\rho C_P)_{nf}} \left(\frac{16\sigma^* T_1^3}{3k^*} \frac{\partial^2 T}{\partial y^2}\right)$$
$$+ \frac{\mu_{nf}}{(\rho C_P)_{nf}} \left(1 + \frac{1}{\beta}\right)\left(\frac{\partial u}{\partial y}\right)^2 + \frac{q'''}{(\rho C_P)_{nf}} + \frac{Q_0}{(\rho C_P)_{nf}} (T - T_0) \quad (11)$$

The temperature of the nanofluid in the channel can be calculated as follows:

$$T_w = T_\infty + B\left(\frac{x}{a}\right)^{m_1} \theta(\eta) \quad (12)$$

The dimensionless form of temperature from Eq. (12) where θ- dimensionless temperature function, η- Similarity variable, m_1 denote the index power-law of the temperature and B is the constant of the fluid.

The pressure gradient of the kind by Vijayalakshmi *et al.* [41]; Bestman [42]; Srinivas *et al.* [43] and Radhakrinshnama charya *et al.* [44] is thought to generate the pulsatile flow.

$$A(1 + ce^{iwt}) = -\frac{1}{\rho_{nf}} \frac{\partial p}{\partial x} \quad (13)$$

By inserting the dimensionless variables and parameters listed below:

$$x = \frac{X}{h}, y = \frac{Y}{a}, t = \omega t', P = \frac{P}{A\rho_{nf}h}, u = \frac{\omega u'}{A}, \theta(\eta) = \frac{T - T_0}{T_1 - T_0} \quad (14)$$

At this moment, we eliminate pressure commencing from equations(12) using (13) and (14) with reference from Vijayalakshmi *et al.* [41] the following is obtained;

$$(1 + ce^{i\omega t}) = -\frac{\partial p}{\partial x} \quad (15)$$

$$\frac{A_2}{A_1 R}(1 + \frac{1}{\beta})\frac{\partial^2 U}{\partial y^2} - \frac{1}{A_1}\frac{\partial p}{\partial x} - \frac{1}{A_1}\left(A_5 M^2 + \frac{A_2}{Da}\right)U - \frac{\partial U}{\partial t} = 0 \quad (16)$$

Eqs(12) using (14) (15) Eqs becomes:

$$\left(\frac{A_4}{A_3} + \frac{4}{3A_3}Rd\right)\frac{1}{R\,\mathrm{Pr}}\theta'' + \frac{A_2}{A_3}\frac{EcA^*}{R}\left(\frac{\partial U}{\partial y}\right)^2 + \frac{B^* Q_H}{A_3 R}\theta - \left(\frac{\partial \theta}{\partial t}\right) = 0 \quad (17)$$

Table 1. Mathematical model for the thermal physical property of a nanofluid

Physical Quantity	Mathematical model
Influential Dynamic viscosity of the nanofluid	$\mu_{nf} = \mu_f (1 - \phi)^{-2.5}$
The influential Density of the nanofluids	$\rho_{nf} = \phi p_s + (1 - \phi) p_f$
The Heat capacitance of nanofluid	$(\rho C_P)_{nf} = \phi (\rho C_P)_s + (1 - \phi)(\rho C_P)_f$
Thermal conductivity of sphericalnanoparticles approximated	$k_{nf} = k_f \left[\frac{2k_f + k_s - 2\phi(k_f - k_s)}{2k_f + k_s + \phi(k_f - k_s)} \right]$
The electrical conductivity	$\sigma_{nf} = \sigma_f \left[1 + \frac{3(\sigma - 1)}{(\sigma + 2) - (\sigma - 1)\varphi} \right]$

Using the following dimensionless similarity variables, where Darcy parameter, the frequency parameter, Eckert number, prandtl number, Heat source parameter, Radiation parameter.

$$Da = \frac{k}{a^2} \ , R = \frac{\omega h^2}{v_f}, Ec = \frac{A^2}{(C_p)_f \omega^2 (T_1 - T_0)}$$

$$\Pr = \frac{(pC_p)_f v_{nf}}{k_f}, Q_H = \frac{Q_0 a^2}{(\rho_{C_f})_f v_f},$$

$$A_1 = \phi \frac{\rho_s}{\rho_f} + (1 - \phi) \ , A_2 = (1 - \phi)^{2.5} \ ,$$

$$A_3 = \phi \frac{(\rho_{cp})_s}{(\rho_{cp})_f} (1 - \phi), Rd = \frac{4T_1^3 \sigma^*}{k_f k^*}$$

$$A_4 = \left[\frac{2k_f + k_s - 2\phi(k_f - k_s)}{2k_f + k_s + \phi(k_f - k_s)} \right]$$

$$A_5 = \left[1 + \frac{3 \left(\frac{\sigma_s}{\sigma_f} - 1 \right) \phi}{\left(2 + \frac{\sigma_s}{\sigma_f} \right) + \left(-\frac{\sigma_s}{\sigma_f} + 1 \right) \varphi} \right] \quad (18)$$

The corresponding boundary conditions are:

$$f(1) = 1, f(-1) = 1, f'(1) = 0, \ and \ f'(-1) = 0. \quad (19)$$

$$\theta(-1) = 1, \theta(1) = 0, if \theta(0) = 1 + \delta\theta'(0) \quad (20)$$

It was once initiated that there is an appropriate settlement between analytical and numerical solutions. Dimensionless shear stress at the partitions is described as heat transfer. The pace of the partitions is a prerequisite for Nusselt quantity non-dimensional, which is characterized by Hatami *et al.* [40]

$$\tau = \frac{x(1 - \phi)^{-2.5}}{R} \left(f''(\eta) \right)_{\eta = -1, 1} \quad (21)$$

$$Nu_x = -\frac{k_{nf}}{k_f} \frac{\partial T}{\partial \eta} / (T_1 - T_0) = -\phi_2 \theta(\eta)_\eta = -1, 1$$
$$C_f = \frac{2\mu_{nf}}{\rho_f(u_w(x))} \left(\frac{\partial u}{\partial y} \right)_{y=0} = -\phi_2 \theta(\eta)_\eta = -1, 1$$
$$q_w = -k_{nf} \frac{\partial T}{\partial y} / y = 0$$

3. Results and Discussion

We investigated in this study the combined property of thermal radiation, heat generation, and viscous dissipation resting on the SWCNT and blood nanofluid flow modal that incorporates nanoparticle volume fraction. Within the numerical computation, the properties of the blood and SWCNT are utilized (reference Table 2). The consistency and accuracy of our accurate solutions and numerical trials of the significant parameters are highlighted through graphs in this section. The governing equation (15) and (16) through the boundary conditions (18) and (19) were worked out by employing the Runge-Kutta strategy through the shooting method (MATLAB solver, bvp4c package software). To achieve these results, mathematical computations are exposed by making an allowance for a distinct norm of non-dimensional governing parameters. The impacts of governing substantial parameters are explored in detail. Specifically; Eckert number(Ec), Magnetic parameter (M), Nanoparticle volume parameter(ϕ), Heat generation parameter (Q_H), Prandtl number (Pr), Darcy number (Da), Casson parameter (β), and A^*, B^* are velocities of heat transfer for the space-dependent; with the following assigned values to the respective parameters: \

$$M = 2, A = 0.5, B = 0.1, m_1 = 0.2, R = 2, Da = 0.5,$$

$$Q_H = 0.1, A^* = 0.2, B^* = 0.2, Nr = 0.5, Ec = 0.2$$

Through Figure 2, the result of A^* on the temperature distribution $\theta(\varsigma)$ is illustrated and from this, we conclude that A^* starts declining against the temperature profile which is being enlarged after a certain range. It is observed from Figure 3 that the impact of B^* on temperature profile $\theta(\varsigma)$ decreases. After these factors, the speed profiles are accelerated. It can be seen from Figure 4 the difference of Eckert number (Ec) through the temperature profile. The incidence of Eckert number in Casson nanofluids enhances the development of thermal vitality, which results in the advance with temperature distributions and in consequence of thermal deposit thickness. The result of the undeniable viscosity of nanofluids supplies vitality from the waft because of the rise in heat electricity through frictional heating and transforms it into interior electricity.

Variations of various heat-generating parameter values are dependent on the temperature; the profile is revealed in Figure.5. When Q_H grows positively, heat production takes up residence in the thermal limit layer. The Casson nanofluid thermal electricity improves due to a large amount of heat. This process raises the thickness of the thermal boundary layer, implying that
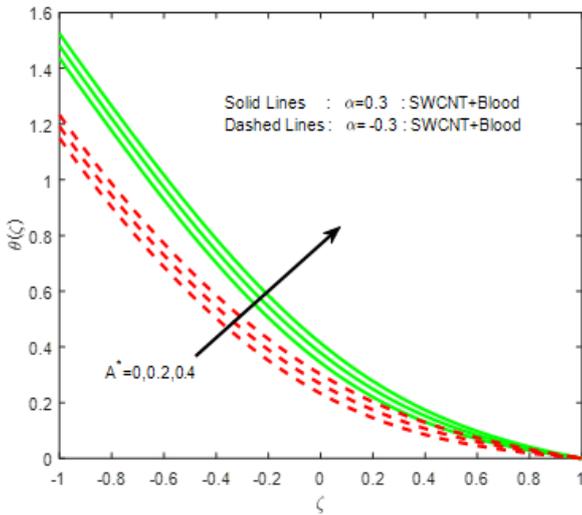
Figure 2. Impact of A^* on $\theta(\varsigma)$
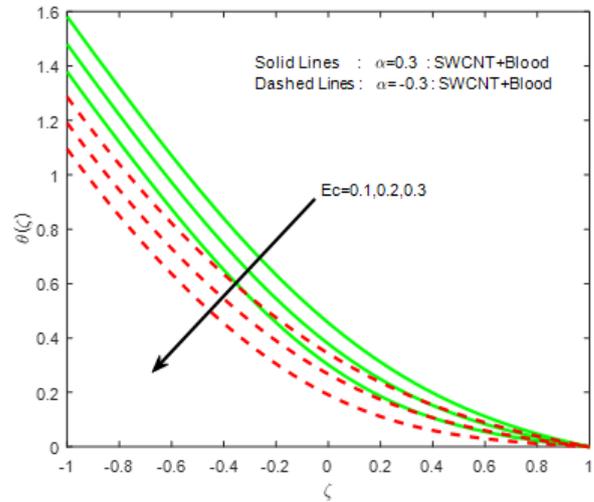
Figure 4. Impact of Ec on $\theta(\varsigma)$
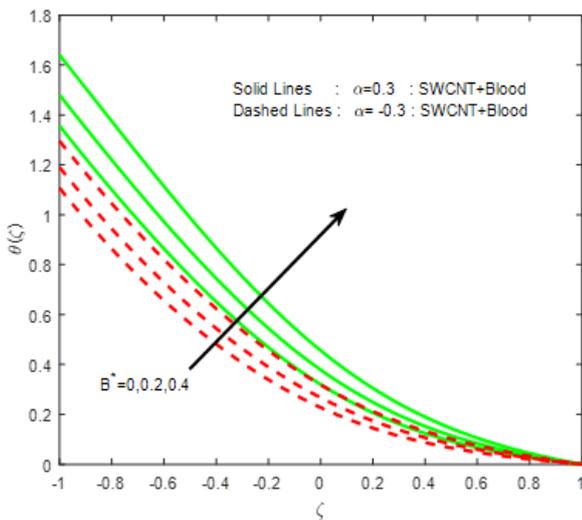
Figure 3. Impact of B^* on $\theta(\varsigma)$
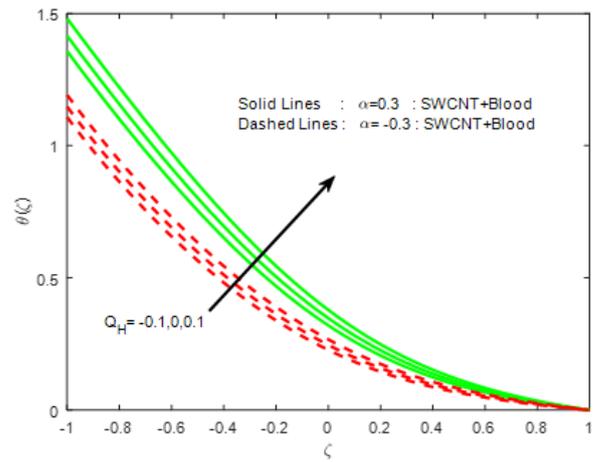
Figure 5. Impact of Q_H on $\theta(\varsigma)$
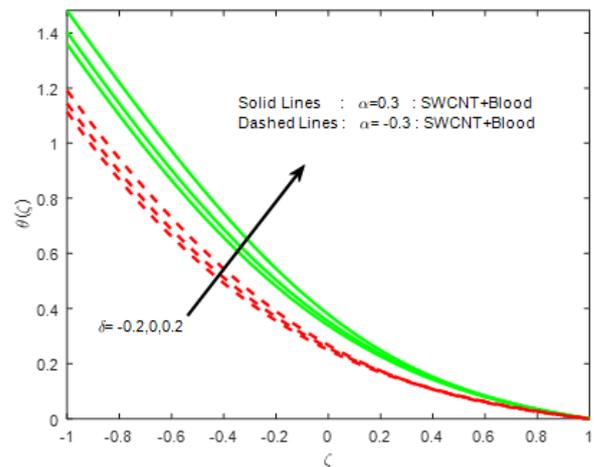
Figure 6. Impact of δ on $\theta(\varsigma)$

warmness strength is activated and, as a result, the temperature of the fluid rises.

The impression of the thermal slip parameter δ on the temperature profile and the velocity profile is depicted through Figure 6. We observed that the thermal slip parameter leads to increases in the temperature distribution and the thermal boundary layer thickness; besides, this outmost impact is noticed at the outside of the channel. Figure 7 shows the impact of the slip parameter on the rate of Casson nanofluid. We noticed that the slip parameter δ at a certain point the velocity of the Casson fluid enhanced.

Figure 8 depicts the effect of Da on velocity profiles of Casson nanofluid, and it is observed that velocity accelerates with rising values of Darcy number. The impact of attractive boundary M on velocity and temperature profiles is shown through Figure 9 and Figure 10. From this, we noticed that the veloc-

Figure 7. Impact of δ on $f'(\zeta)$
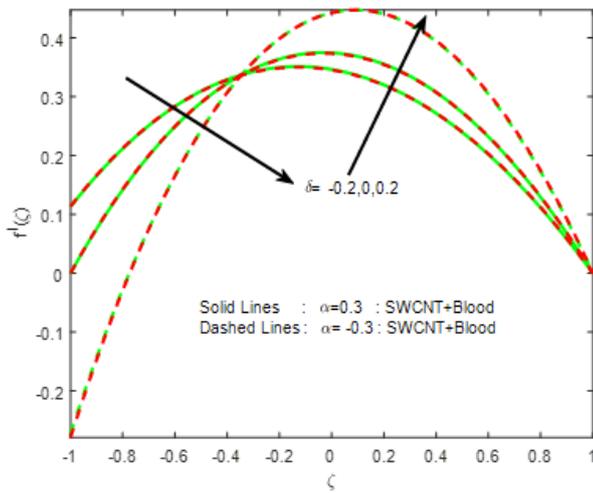
Figure 9. Impact of M on $f'(\zeta)$

Figure 8. Impact of Da on $f'(\zeta)$
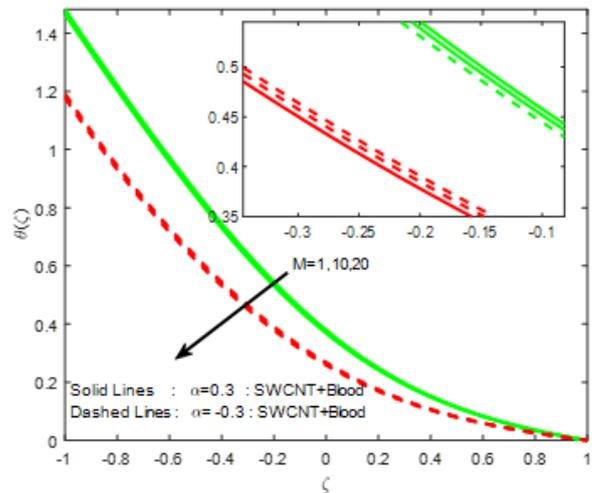
Figure 10. Impact of M on $\theta(\varsigma)$

ity profiles decline for SWCNT with rising values of M resulting thickness of the boundary layer is reduced at a faster rate. Physically, the Lorentz energy, which opposes movement, occurs due to the used transverse magnetic flow and is responsible for reducing fluid velocity. Besides, as the temperature profiles are improved, the temperate limit layer thickness expands.

The impact of blood parameters β on the velocity and temperature distributions is shown in Figure 11 and Figure 12; it is noticed that for the increasing value of β, the velocity profile decreases for SWCNT. It is because of blood with β will increase the plasticity of blood fluid expands with motive the deceleration in velocity. It's due to the blood's malleability, when β decreases, the flexibility of the fluid increases, causing the pace to slow down. In addition, the temperature profile of the flow escalates for increasing values of M.

In Figure 13, the impact of volume fraction ϕ on the temperature profile for human blood-based nanofluid with SWCNT is displayed; it is noticed that for both human blood flow and SWCNT, as the ϕ rises, the temperature of the nano-fluid also increases. It is additionally referred to as those changes in ϕ in-

dicating the adjustments in temperature after which shows the significance of nanofluid.

The impact of A on velocity and temperature profiles are portrayed through Figure 14 and Figure 15; it is noticed that the temperature profile $\theta(\varsigma)$ escalates and the velocity profile $f'(\zeta)$ decelerates with the impact of A.

In Figure 16, the outcomes of the m_1 on the temperature profile are displayed; the temperature of the nanofluid decreases to SWCNT with increasing value of m_1, which leads to a decline in velocity boundary deposit thickness.

3.1. Physical Properties of Base Fluid and Nano-Particles

Thermo substantial properties regarding the base fluid and nanoparticles of carrier fluid human blood and SWCNT nanoparticles are given below Table 2

3.2. Skin Friction and Nusselt Number for the Cases of Unsteady Contraction/Expansion

From Table 3 it is seen that the coefficients of space with temperature-dependent A^* and B^* with relatively high-temperature

Table 2. Physical properties of Base fluid & Nanoparticles (Blood and SWCNT)

Physical properties	Solid Nanoparticles SWCNT	Base fluid blood
c_p(j/kg k)	425	3617
κ(w/m k)	6600	0.52
ρ (kg/m^3)	2600	1050
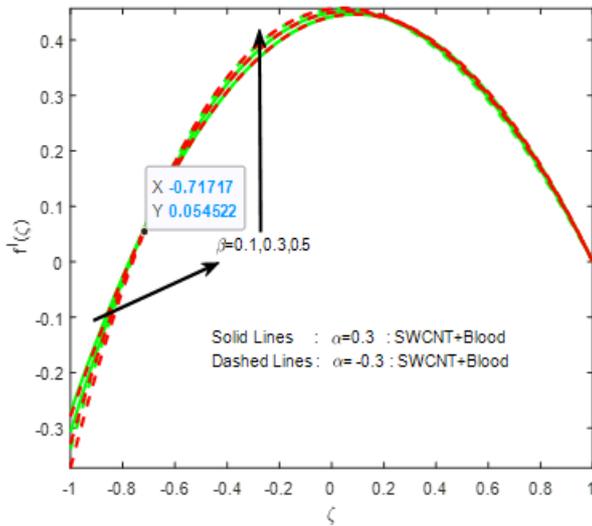
Figure 11. Impact of β on $f'(\zeta)$
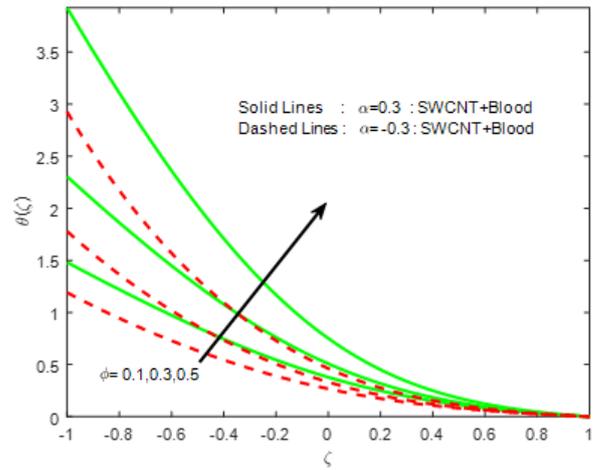
Figure 13. Impact of ϕ on $\theta(\varsigma)$
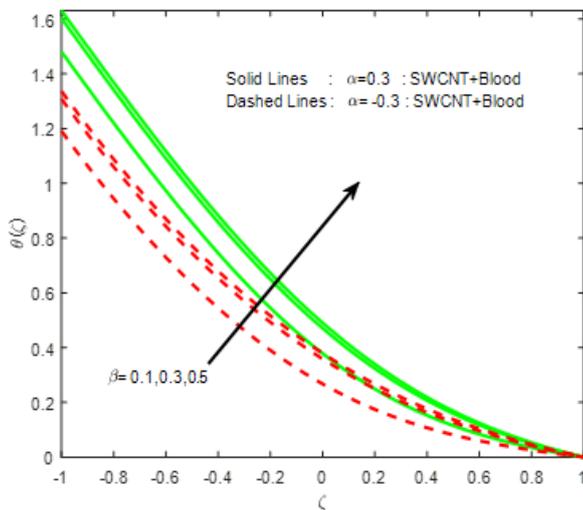
Figure 12. Impact of β on $\theta(\varsigma)$
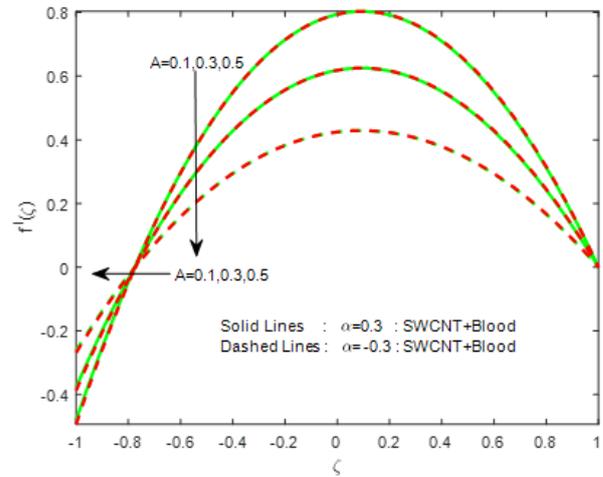
Figure 14. Impact of A on $f'(\zeta)$

source/sink, the skin friction coefficient stable in nature whereas the Nuselt number will be enhanced. With the improved values of Da, both skin friction and Nusullt number decrease. The enhanced values βreduce skin friction on velocity, in addition, to enhancing the heat transfer moderately. The pores of skin friction remain stable, convenient and incomplete gradual reduction inside heat transfer velocity used with increasing values ofNr &Q_H. In this case of M, friction (C_f)and Nusselts num-

ber decrease. For the effect of the parameters Ec, ϕ and$A$, both the values of skin friction, Nusselts number declines, whereas form_1, both skin friction and Nusselt number increases.

3.3. Skin Friction and Nusselt Number for Steady Contraction Situation

In the above Table 4, we can see that the enhanced values of A^*as well as B^*have no impact resting on skin friction, although these values concentrated the heat transfer velocity. The skin friction values for the variations in Daremained constant whereas local Nusselt number values will be increasing. The enhanced values of β covers the oscillatory nature for pores

Table 3. The impact of various parameters on skin friction(C_f) and Nusselt number (Nu_x) for the cases of unsteady contraction/expansion

A^*	B^*	Da	β	Nr	Q_H	M	Ec	δ	ϕ	A	m_1	C_f	Nu_x
0.0												19.471388	3.193296
0.2												19.471388	3.290621
0.4												19.471388	3.387946
	0.0											19.471388	3.015712
	0.2											19.471388	3.290621
	0.4											19.471388	3.646890
		0.001										66.175569	3.259443
		0.05										24.559828	3.307261
		0.1										21.627181	3.298364
			0.1									19.471388	3.290621
			0.3									8.683747	3.562513
			0.5									6.435490	3.624260
				0.5								19.471388	3290621
				1.0								19.471388	5.542735
				1.5								19.471388	7.858197
					-0.1							19.471388	3.015712
					0.0							19.471388	3.144902
					0.1							19.471388	3.290621
						1						19.246748	3.292558
						10						21.302554	3.274551
						20						23.677717	3.252965
							0.1					19.471388	3.516654
							0.2					19.471388	3.290621
							0.3					19.471388	3.064588
								-0.2				8.072545	3.021844
								0.0				11423853	3.118250
								0.2				19.471388	3.290621
									0.1			19.471388	3.290621
									0.3			35.873231	8.780344
									0.5			19.180772	27.79143
										0.1		34.402685	4.064004
										0.3		27.006243	3.661321
										0.5		18.710125	3.254065
											0.0	19.471388	3.267488
											1.0	19.471388	3.401005
											2.0	19.471388	3.579480

and skin friction although there is an insignificant variation for heat transfer rate. Influence of m is not affecting skin friction whereas heat transfer velocity is decreased for the same m values. There is an oscillatory characteristic in pores and skin friction and a fast increased within the heat transfer velocity which is meant for rising values of A. Raising values of the slip parameter ϕ escalate the both skin friction and Nusselt number. For the influence of m_1, the skin friction values remain constant and the local Nusselt number decrease.

4. Validation

Similarly, Table 4 is organized to explain Nu at the employing the Runge-Kutta strategy through the shooting method estimated for different values of relevant model variables for both SWCNTs and MWCNTs Nano fluids. From Table 3 and Table 4, it can be observed that the weight of rate of heat transport accelerates for a high magnitude of both ϕ and Pr and declines for a higher value of the Eckert number (Ec). Eckert number (Ec) is related to the dissipation term, and the more considerable importance of Eckert number (Ec) enhances the thermal field. Therefore, the opposite result for the higher significance of the Eckert number (Ec) verses Nu is perceived Table 5

5. Conclusion

In this article, the stagnation flow on SWCNT and blood nanofluids of MHD fluid in the existence of a porous medium, viscous dissipation, and injection/suction in addition to thermal radiation parameters are studied and analyzed through this examination. The resulting equations were solved by numerical techniques. The tables and graph values for the tempera-

Table 4. The impact of various parameters on skin friction (C_f) and Nusselt number (Nu_x) for steady contraction situation

A^*	B^*	Da	β	Nr	Q_H	M	Ec	δ	ϕ	A	m_1	C_f	Nu_x
0.0												19.997073	2.555168
0.2												19.997073	2.647360
0.4												19.997073	2.739552
	0.0											19.997073	2.462266
	0.2											19.997073	2.647360
	0.4											19.997073	2.880635
		0.001										68.577628	2.542118
		0.05										25.222523	2.654748
		0.1										22.208947	2.651121
			0.1									19.997073	2.647360
			0.3									9.274754	2.907525
			0.5									7.085115	2.970431
				0.5								19.997073	2.647360
				1.0								19.997073	4.751474
				1.5								19.997073	6.972890
					-0.1							19.997073	2.462266
					0.0							19.997073	2.549819
					0.1							19.997073	2.647360
						1						19.769175	2.649027
						10						21.854765	2.633497
						20						24.264288	2.614779
							0.1					19.997073	2.860118
							0.2					19.997073	2.647360
							0.3					19.997073	2.434603
								0.2				8.119202	2.475313
								0.0				11.560063	2.542268
								0.2				19.997073	2.647360
									0.1			19.997073	2.647360
									0.3			36.522610	6.779180
									0.5			91.966641	20.72406
										0.1		35.32447	3.026218
										0.3		27.732563	2.846351
										0.5		19.215453	2.625739
											0.0	19.997073	2.765707
											1.0	19.997073	2.328076
											2.0	19.997073	2.100096

Table 5. The numerical values of the Nusselt number $-\phi'(1)$

Pr	Ec	ϕ	$-\phi'(1)$	
			SWCNTs	MWCNTs
20	1.5	0.01	0.067257	0.201779
21			0.107184	0.254538
22			0.127169	0.307473
20	1.6		0.067655	0.202565
	1.6		0.068047	0.203369
	1.5	0.02	0.246742	0.517264
		0.03	0.427643	0.835802

ture field, skin-friction coefficient, velocity profiles, local Nusselt number with the effects of parameters magnetic enclosure thermal radiation, thermophoresis, Prandtl number, permeability parameter, and Eckert number are exposed and obtained. The numerous observations of the current examined about the following conclusions.

1. Human blood as well as the base fluid is drastically utilised first time to attain the solution for Casson nano-fluids. It's extremely noticed that rate decreases with increasing CNT quantity portion, and advances in CNT quantity division will increase the blood temperature, which affects in and gives an improvement to the heat transfer velocity.

2. The velocity expressed increases through increasing the velocity fraction parameter about the temperature and concentration profiles are decreased and increased by A.

3. An increase of the SWCNT solid ϕ quantity section and Eckert quantity yields an addition with nano-fluids tem-
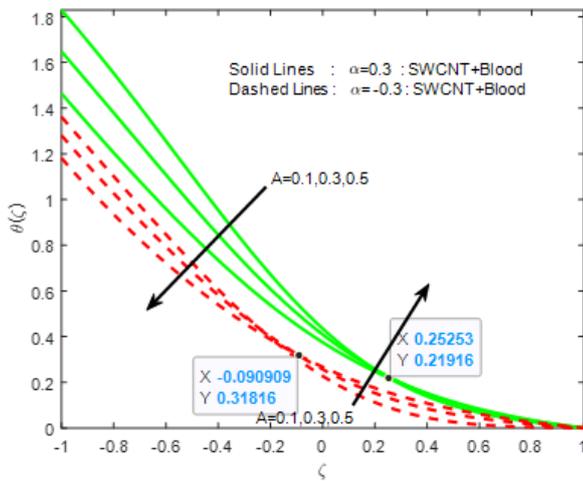
Figure 15. Impact of A on $\theta(\varsigma)$
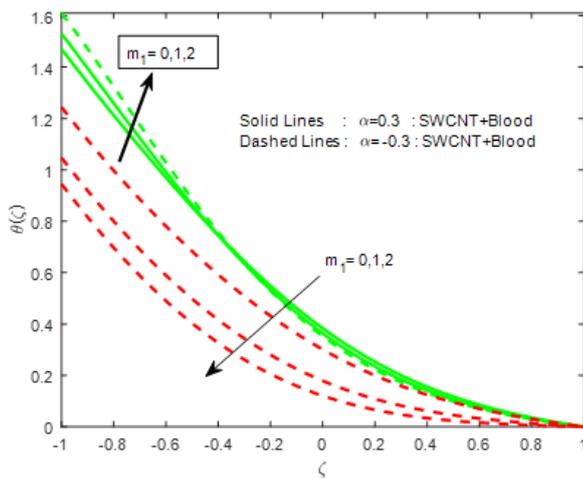
Figure 16. IImpact of m_1 on $\theta(\varsigma)$

perature, leading to the direction of sudden radiation in the heat transfer rates.

4. Increasing values of the slip parameterδreduces the pace subject. The concept of base fluid provides parameter enhancement in the temperature.

5. The viscous dissipation affects the flow within the temperature profile and decreases with the insignificant value of the (Pr)Prandtl quantity.

6. An Eckert number (Ec)shows a small effect C_f decreased but Nu_x has increased with the enlargement of the (Ec) Eckert number. The temperature distribution $\theta(\eta)$ is increased as the Eckert number (Ec) and Radiation parameter increase.

7. The thermal radiation, heat generation/absorption, and permeability parameters throughout decreases with ad-

vancement in prenatal number, the unsteadiness, the suction, and the magnetic parameter.

8. As an essential position in dissipating heat the temperature of the fluid decreases through enhancement with nanoparticle quantity section for SWCNT as a result of elevated thermal conductivity. An expansion in the SWCNT's quantity suction increases the Casson-nanofluid temperature, which affects inflation in the heat transfer velocity.

9. SWCNTs hold an identical consequence resting on the velocity with temperature profiles for Casson nanofluid flow. The resistance impedance in the direction of flow confirms higher results used for the SWCNT case than for the pureblood case.

Acknowledgement

References

[1] N. J. Salman Ahmed., T. M. Yunus Khan, Sarfaraz Kamangar & Azeem, "Effect of viscous Dissipation and radiation in an annular cone", AIP Conference Proceedings **1751** (2016).

[2] S. P. Anjali Devi & D. Vasantha Kumara., "Thermal radiation, viscous dissipation, ohmic dissipation, and mass transfer effects on unsteady hydromagnetic flow over a stretching surface", Ain Shams Engineering Journal **9** (2018) 1161.

[3] M. Abd El Aziz, "Thermal diffusion and diffusion thermo effects on combined heat and mass transfer hydromagnetic three-dimensional free convection flow over a permeable stretching surface with radiation", Phys Lett. A .**372** (2007) 263.

[4] S. P. Anjali Devi & M. Kayalvizhi, "Analytical solutions of MHD flow with radiation over a the stretching sheet is embedded in a porous medium", Int J Appl Math. **6** (2010) 82.

[5] O. D. Makinde & P. Sibanda, "Effects of chemical reaction on boundary layer flow past a vertical stretching surface in the presence of internal heat generation", Int J Numer Math Heat Fluid Flow **21** (2011) 779.

[6] Y. I. Seini & O. D. Makinde, "MHD boundary layer due to the exponentially stretching surface with Radiation and chemical reaction", Math Prob Eng. **7** (2013).

[7] A. K. Abdul Hakeem, R. Kalaivanan, N. Vishnu Ganesh & B. Ganga, "Effect of partial slip on hydromagnetic flow over a porous stretching sheet with non-uniform heat source/sink, thermal radiation, and wall mass transfer", Ain Shams Eng J. **5** (2014) 913.

[8] C. K. Chen, M. I. Char, "Heat transfer of a continuous stretching surface with suction or blowing", J Math Anal. **135** (1988) 568.

[9] K. Bhagya Lakshmi, G.S.S. Raju, P.M. Kishore & N. V. R. V. Prasada Rao, "The Study of heat generation and viscous dissipation on MHD heat And mass diffusion flow past a surface", IOSR Journal of Applied Physics (IOSR-JAP) **5** (2013) 17.

[10] C. S. K. Raju & N. Sandeep, "MHD slip flow of a dissipative Casson fluid over a moving geometry with heat source/sink: a numerical study", Acta Astronautica **133** (2017) 436.

[11] S. Suneetha, N. Bhaskar Reddy and V. Ramachandra Prasad, "The thermal radiation effects on MHD free convection flow past an impulsively started vertical plate with variable surface temperature and concentration", Journal of Naval Architecture and Marine Engineering **5** (2008) 57.

[12] H. Kumar, "Radiative heat transfer with hydromagnetic flow and viscous dissipation over a stretching surface in the presence of variable heat flux", Thermal Science **13** (2009) 163.

[13] S.A.Al-Sanea, "Mixed convection heat transfer along with a continuously moving heated vertical plate with suction or injection", International Journal of Heat and Mass Transfer **47** (2004) 1445.

[14] H. S. Takhar., S. Roy & G. Nath, "Unsteady free convection flow over an infinite vertical porous plate due to the combined effects of thermal and mass diffusion, magnetic field and Hall currents", Heat and Mass Transfer **39** (2003) 825.

[15] R.Cortell, "Suction, viscous dissipation and thermal radiation effects on the flow and heat transfer of a power-law fluid past an infinite porous plate", Chemical Engineering Research and Design **89** (2011) 85.

[16] B. K. Jha, A. K. Samaila & A. O. Ajibade, "Unsteady/steady natural convection flow of reactive viscous fluid in a vertical annulus", International Journal of Fluid Mechanics Research **39** (2012) 301.

[17] M. Shamshuddin., S. R. Mishra O., Anwar Bég A. Kadir, "Viscous dissipation and Joule heating effects in non-Fourier MHD squeezing flow, heat and mass transfer between riga plates with thermal radiation: variational parameter method solutions", Arabian Journal for Science and Engineering **5** (2019) 8053.

[18] Z. Shah, P. Kumam & W. Deeban., "Radiative MHD Casson Nanofluid flow with activation energy and chemical reaction over past nonlinearly stretching surface through entropy generation", Scientific Reports **10** (2020).

[19] S. Reddy, K. Naikoti & M. M. Rashidi, "MHD flow and heat transfer characteristics of Williamson nanofluid over a stretching sheet with variable thickness and variable thermal conductivity", Transactions of Razmadze Mathematical Institute **171** (2017) 195.

[20] T. Hayat, S. A. Shehzad & A. Alsaedi, "Soret and Dufour effects on magneto Hydrodynamic (MHD) the flow of Casson fluid", Applied Mathematics and Mechanics (English Edition) **33** (2012) 1301.

[21] F. Ali, N. A. Sheikh., I. Khan & M. Saqib, "Magnetic field effect on blood flow of Casson fluid in an axisymmetric cylindrical tube: a fractional model", Journal of Magnetism and Magnetic Materials **423** (2017) 327.

[22] A. Dawar, Z. Shah, W. Khan, M. Idrees & S. Islam, "Unsteady squeezing flow of magnetohydrodynamic carbon nanotube nanofluid in rotating channels with entropy generation and viscous dissipation", Advances in Mechanical Engineering **11** (2019).

[23] K. A. Kumar, J. V. Reddy, V. Sugunamma & N. Sandeep, "Simultaneous solutions for MHD flow of Williamson fluid over a curved sheet with non-uniform heat source/sink", Heat Transfer Research **50** (2019) 581.

[24] C. Sus., "Enhancing thermal conductivity of fluids with nanoparticles", International Mechanical Engineering Congress and Exposition **66** (1995) 99.

[25] R.U. Haq, S. Nadeem, Z. H. Khan & N. F. M. Noor, "Convective heat transfer in MHD slip flow over a stretching surface in the presence of carbon nanotubes", Physica B: Condensed Matter **457** (2015) 40.

[26] M. S. Liu, M. Ching-Cheng Lin., I. T. Huang & C. C. Wang, "Enhancement of thermal conductivity with carbon nanotube for nanofluids", International Communications in Heat and Mass Transfer **32** (2005) 1202.

[27] S. Nadeem & C. Lee, "Boundary layer flow of nanofluid over an exponentially stretching surface", Nanoscale Research Letters **94** (2012).

[28] A. Bejan, "Second law analysis in heat transfer", Energy **5** (1980) 720.

[29] T. Hayat, M. Rafiq, B. Ahmad & S. Asghar, "Entropy generation analysis for peristaltic flow of nanoparticles in a rotating frame", Int. J. Heat Mass Transf. **108** (2017) 1775.

[30] D. Nouri, M. Pasandideh-Fard, M. J. Oboodi, O Mahian & A. Z. Sahin, "Entropy generation analysis of nanofluid flow over spherical heat source inside a channel with sudden expansion and contraction", Int. J.Heat Mass Transf. **116** (2018) 1036.

[31] S. Das, A. S. Banu, R. N. Jana & O. D. Makinde, "Entropy analysis on MHD pseudo-plastic nanofluid flow through a vertical porous channel with convective heating", Alexand. Eng. J. **54** (2015) 325.

[32] M. Sheremet, I. Pop, H. F. Oztop & N. Abu-Hamden, "Natural convection of nanofluid inside a wavy cavity with non-uniform heating: Entropy generation analysis", Int. J. Numer. Math. Heat Fluid Flow **27** (2017) 958.

[33] S. O. Alharbi, A. Dawar, Z. Shah, W. Khan, M. Idrees, S. Islam & I. Khan, "Entropy Generation in MHD Eyring–Powell fluid flow over an unsteady oscillatory porous stretching surface under the impact of thermal radiation and heat source/sink", Appl. Sci. **8** (2018).

[34] Z. Jordan & J. Network, "Simulation method applied to radiation and dissipation effects on MHD unsteady free convection over vertical porous plate", Applied Mathematical Modelling **31** (2007) 2019.

[35] S. Uchida & H. Aoki, "Unsteady flows in a semi-infinite contracting or expanding pipe", Journal of Fluid Mechanics **82** (1977) 371.

[36] E. C. Dauenhauer & J. Majdalani, *Unsteady flows in semi-infinite expanding channels with wall injection*, AIAA (1999).

[37] J. Majdalani & C. Zhou, "Moderate-to-large injection and suction driven channel flows with expanding or contracting walls", Journal of Applied Mathematics and Mechanics **83** (2003) 181.

[38] S. Xin-Hui, Z, Liacun, Z. Xinxin & S. Xinyi, "Homotopy analysis solutions for the asymmetric laminar flow in a porous channel with expanding or contracting walls", Acta Mechanica Sinica **27** (2011) 208.

[39] M. Q. Brewster, *Thermal Radioactive transfer and properties*, Wiley, New York (1992).

[40] M, Hatami, M, Sheikholeslami & D. D, Ganji, "Nanofluid flow and heat transfer in an asymmetric porous channel with expanding or contracting walls", Journal of Molecular Liquids **195** (2014) 230.

[41] A. Vijayalakshmi, S. Srinivas, B. Satyanarayana & A. Subramanyam Reddy, "The hydromagnetic pulsating flow of nanofluid between two parallel walls with a porous medium", Materials Today: Proceedings **9** (2019) 306.

[42] A. R. Bestman, "Pulsatilr flow in heated porous channel", Int. J. Heat Mass Transfer 25 (1982) 675.

[43] S. Srinivas, T. Malathy & P. L. Sachdev, "On pulsatile hydromagnetic fow of an Oldroyd fuid with heat transfer", Eng. Trans. **55** (2007) 79.

[44] G. Radhakrishnamacharya, & M. K. Maiti, "Heat transfer to pulsatile flow in a porous channel", Int. J. Heat Mass Transfer **20** (1977) 171.

[45] H. T. Alkasasbeha, M. Z. Swalmeh, H. G. Bani Saeed, F. M. Al-Faqih & A. G. Talafha, "Investigation on cnts-water and human blood-based Casson nanofluid flow over a stretching sheet under the impact of the magnetic field", Frontiers in Heat and Mass Transfer (FHMT) **14** (2020) 1.

[46] N. A. Zainal, R. Nazar, K. Naganthran & I. Pop. "Magnetic impact on the unsteady separated stagnation-point flow of hybrid nanofluid with viscous dissipation and joule heating", Computational and Applied Mathematics 10 (2022).

[47] N. A. Zainal, R. Nazar, K. Naganthran & I. Pop. "Viscous dissipation and MHD hybrid nanofluid flow towards an exponentially stretching/shrinking surface", Neural Comput & Appl. **33** (2021) 11285.

[48] T. Gul, J. ur Rahman, M. Bilal, A. Saeed, W. Alghamdi, S. Mukhtar, H. Alrabaiah & E. Bonyah. "Viscous dissipated hybrid nano liquid flow with Darcy–Forchheimer and forced convection over a moving thin needle", AIP Advances **10** (2020).

[49] A. K. Pati, A. Misra & S. K. Mishra, "Effect of electrification of nanoparticles on heat and mass transfer in boundary layer flow of a copper water nanofluid over a stretching cylinder with viscous dissipation", JP Journal of Heat and Mass Transfer **17** (2019) 97.

[50] O. Adedire & J. N. Ndam, "Mathematical modelling of concentration profiles for species transport through the single and the interconnected multiple-compartment systems", J. Nig. Soc. Phys. Sci. **2** (2020) 61.

[51] M. Ramanuja, B. T. Raju, V, Nagaradhika, R. B. Madhusudhana, P. Durgaprasad & C. S. K. Raju, "Significance of Axisymmetric Flow of Casson Darcy Unsteady Slip Flow in a Suspension of Nanoparticles with Contracting Walls". Journal of Nano-fluids **11** (2022) 350.

[52] H. C. Brikman, "The viscosity of concentrated suspensions and solutions", Journal of Chemical Physics **20** (1952) 571.

[53] R. I. Hamilton, O. K. Crosser, "Thermal conductivity of heterogeneous two-componentSystem", I and EC Fundamentals **1** (1962) 187.

[54] M. Kida, S. Adam, O. O. Aduroja & T. P. Pantuvo, "Numerical solution of stiff and oscillatory problems using third derivative trigonometrically fitted block method",.J. Nig. Soc. Phys. Sci. **4** (2022) 34.

Appendix

u & v Fluid flow velocity

μ Dynamic viscosity

ρ Density of the fluid

ρ_s - be the density of the nanoparticle,

p Dimensional pressure

β Blood Casson fluid parameter

k_{nf} Thermal conductivity

μ_f - viscosity of the base fluid

k_f; k_s Thermal conductivities

ρ_{nf} Efficient density of the nanofluid

$(\rho_{C_P})_{nf}$ Heat electrical condenser of the nanofluid

v Kinematic viscosity

k_f; k_s Thermal conductivities

T fluid temperature

K Porous permeability

R Radiation

Da Darcy Number

λ_1 Jeffrey parameter

θ Dimensionless temperature